Please note: While FORCE appreciates the significant work involved in this study, subsequent review by our science team has identified substantial analytical errors, listed below, that invalidate the results of this study and their subsequent interpretation. This report should not be referenced, nor form the basis of other work. It remains in our document collection only for archival purposes. Interested readers are encouraged to review a related, more recent report (completed 2019), found here.

Methodological errors:

- Instrument calibration settings were invalid because of calibration data acquisition procedures adopted during field operations, and inadequate quality control of calibration analytical processes afterwards.

- Standard data quality controls and data processing procedures were not followed leading to incorrect values being included in the analysis.

- Substantial analytical and computer coding errors were made in the way that tide phases, diel states, and “with” and “against” were assigned to the data and reported in the document.

- Data was mislabelled and errors were made in the way that data was aggregated (e.g., differing-sized integration bins), with some data being duplicated in the dataframe used for analysis.

- Hydroacoustic post-processing software was not certified for use with the EK80 echosounder data (automated warnings generated by the software were ignored).

Louise P. McGarry, PhD
Hydroacoustician

Daniel J. Hasselman, PhD
Science Director

Fundy Ocean Research Center for Energy (FORCE)

Final report

Marine Fish Monitoring Program Tidal Energy Demonstration Site – Minas Passage

Submitted to the Fundy Ocean Research Center for Energy (FORCE)

Prepared by: Aurélie Daroux and Gayle Zydlewski

University of Maine
School of Marine Sciences

Contact information:
gayle.zydlewski@maine.edu
207-581-4365

Submitted: 21 June 2017

Comments received: 11 September 2017

Final Edits: 16 October 2017

This is the final report submitted = to the Fundy Ocean Research Center on Energy (FORCE) for the *Marine Fish Monitoring Program Tidal Energy Demonstration Site – Minas Passage*. It includes a description of the survey design, the methodology used to process and analyze the data, the results and their interpretation for 2016 and 2017.

Summary: Six 24-hour hydroacoustic surveys were run successfully, three before the turbine deployment (May, August and October 2016) and three after (November 2016, January and March 2017). Data processing methods were implemented to export relative fish density while removing noise created by entrained air. Historical (2011-2012) data supplied by Gary Melvin, Canadian Department of Fisheries and Oceans, was re-processed and relative fish density was combined with the 2016-2017 data to complete the dataset.

Mean relative fish densities were variable, with higher relative densities observed in the Crown Lease Area site (turbine site) where the turbine berths are located compared to the reference site (across the channel). The highest relative density was observed in May 2016 and may have been associated with the alewife and striped bass spring spawning migrations as well as the presence of Atlantic herring. During winter surveys (November and January, all years), relative fish density was also high compared to other months, possibly reflecting different fish behavior in different parts of the channel during that time of year.

Fish vertical distribution, from bottom to surface, varied greatly within and among surveys. We estimate that the percentage of fish at the depth of the OpenHydro turbine (based on data collected adjacent to the turbine) also varied greatly and ranged between 2 and 51% depending on the time of year.

Our results did not show a significant effect of the turbine (during the three surveys it was present) in the mid-field on overall relative fish density or any obvious change in vertical distribution in the water column. However, statistical comparisons were limited because the turbine was only present in the site for restricted periods of time. As such, monitoring of the region should continue to assess changes in fish distribution over time.

In summary, a valid approach to monitoring the regional responses to changes in the CLA has been developed and should be used moving forward. We recommend that similar monitoring continue in order to assess changes in fish distribution patterns as the site is further developed; ideally, physical sampling of fish be conducted to verify the presence of species seasonally; and a complete probability of encounter model would require concentrated transects over-the-turbine.

Contents

Glossary

Area backscatter (Sa or sa): Total area backscatter (Sa in dB or sa in $m^2 \cdot m^{-2}$) is volume backscatter integrated over depth, and therefore scales to 1 m^2. Sa from different depth layers can be used to estimate the **vertical distribution** of fish.

Bin**:** analysis cell used for echo integration, with horizontal units in distance or time and vertical (depth) units in distance.

CLA: Crown lease area at FORCE site in Minas Passage, where Tidal In-Stream Energy Conversion (TISEC) devices can be connected to one of five berths.

Contemporary data: dataset collected by FORCE and the University of Maine in 2016 and 2017.

Echosounder: a device which uses the sound properties in water for the measurement of underwater biological components.

Echo integration**:** Echo integration is a widely-adopted and well-established technique for estimatingacoustic target density and hence biomass from hydroacoustic data. Echo integration can be run using vertical (depth) and/or horizontal (time or distance) bins.

FORCE: Fundy Ocean Research Center for Energy.

GLM: generalized linear model, the application of regression models to explain the relationships between a response variable (e.g., sv) as a function of other parameters/features (e.g., tide).

GR1_N0A (transect naming convention): this naming convention was used to identify the grid (GR1 to GR4), transect (N0 to N5 for CLA transects, S1 to S3 for reference site transects), and the direction the vessel was moving relative to the tide (W = with, A = against). Example: GR1_N0A is for grid 1 (first grid of the survey), transect N0, run against the tide.

Grid: The series of transects carried out at the CLA and reference sites over the course of one tidal stage (e.g., ebb or flood).

Historical data: dataset collected by Gary Melvin in 2011 and 2012 and described in (Melvin and Cochrane 2014).

Mid-field*:* approximately 100 m distance from a turbine.

Near-field: within 100 m of a turbine.

ORPC: Ocean Renewable Power Company.

Outliers: data values that differ greatly from the majority of a set of data. These values fall outside of an overall trend that is present in the data.

Site: A physical location where data are collected. The CLA site was on the north side of the Minas Passage, and the reference site defined for these surveys was on the south side of the passage.

Survey: a 24-hour period of time during which acoustic data are collected at the CLA and reference sites. Each survey includes four complete grids (one during each tidal stage at each the CLA and reference sites). Six surveys were carried out in 2011-2012 (historical data) and six in 2016-2017 (contemporary data).

Transect: The individual lines traversed by the vessel across the CLA and reference sites, with and against the current. During contemporary surveys six transects were carried out at the CLA (named N0 to N5), and three were carried out at the reference site (named S1 to S3). In the historical dataset there were 9 transects in the CLA and 1 in the reference site.

TISEC: Tidal In-Stream Energy Conversion

Volume backscatter, water column relative fish density (Sv, and sv): Volume backscatter (Sv in dB or sv in $m^2 \bullet m^{-3}$) is the summation of the acoustic energy reflected by all targets within a sampling volume, scaled to 1 m^3. Alone, volume backscatter is a relative measure of the density of acoustic targets. When combined with species composition (if known), volume backscatter can be used to estimate absolute fish density and abundance (McLennan and Simmonds, 2013). In this report, volume backscatter is used as Sv (dB value) and sv (linear value) in plots and as relative fish density in the main text.

Introduction

The Bay of Fundy has the largest tides in the world. The Fundy Ocean Research Center for Energy (FORCE) has created a facility in Minas Passage to allow industry to demonstrate and evaluate tidal in-stream energy conversion (TISEC) technology. FORCE is required to establish an Environmental Effects Monitoring Program (EEMP) covering device mid-field effects on fish, lobsters, marine birds, marine mammals, and marine noise. This document specifically addresses the EEMP for fish in the area that includes the FORCE Crown Lease Area (CLA). On November 8, 2016, a turbine was deployed in berth D of the FORCE CLA (Fig 1).

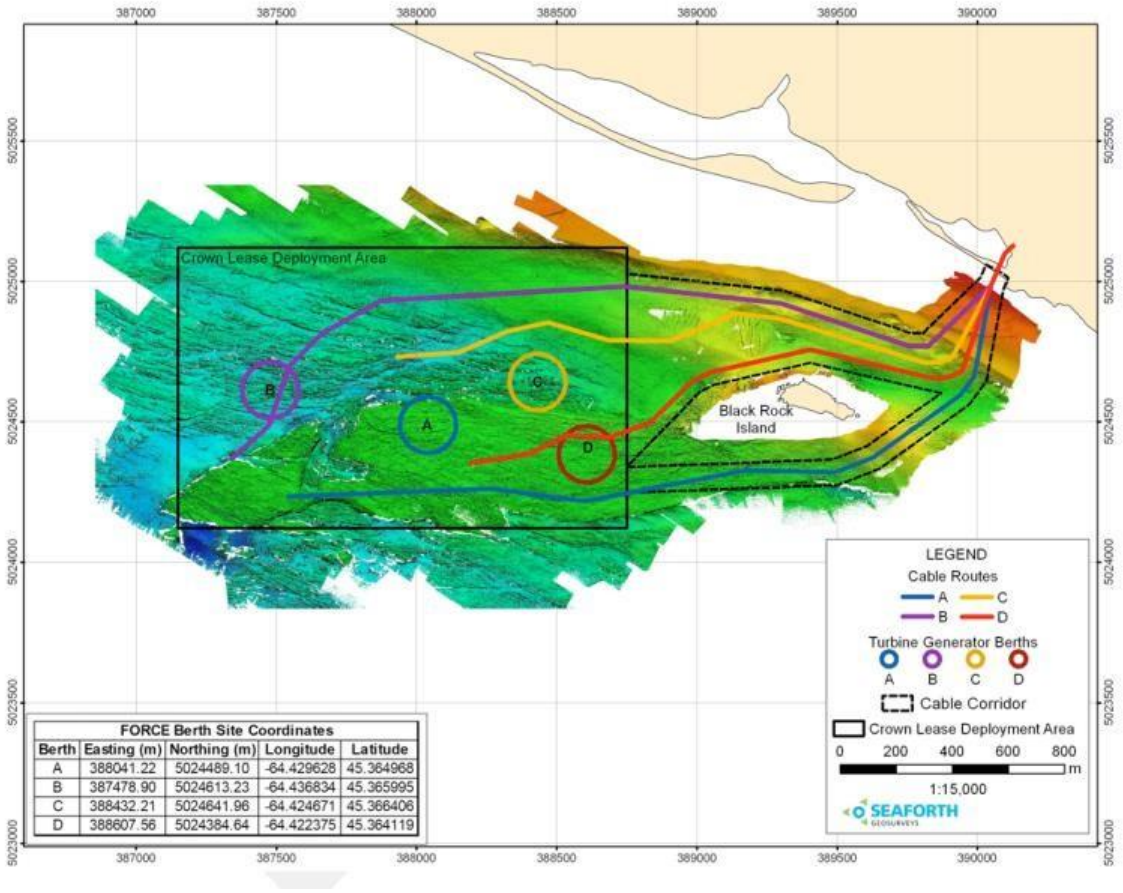

Figure 1: Crown Lease turbines deployment Area map. The turbine was deployed in berth D.

This project was designed to assess indirect effects of deployed TISEC devices in the FORCE CLA by quantifying fish behavior changes, measured as changes in spatial distribution in the mid-field (i.e., 100-1000 m from the turbine). Indirect effects are changes in the mid-field of the turbine that are associated with turbine presence and do not include direct interaction with the turbine in its near-field. Specific objectives included: (1) testing for indirect effects of TISEC devices on relative fish density throughout the entire water column; (2) testing for indirect effects of TISEC devices on fish vertical distributions; and (3) estimating the probability of fish being at the same depth of the turbine based on the vertical distribution of fish relative to a deployed TISEC device depth.

Logistical difficulties and safety considerations in tidally dynamic regions can be barriers to performing quantitative fisheries surveys using physical capture of fish. As such, project objectives were accomplished using mobile surveys with a down-looking hydroacoustics echosounder (EK80) mounted to a medium-sized boat (the *Nova Endeavor*) using field methods, data processing, analysis techniques, and interpretation that were applied at the

successful ORPC Cobscook Bay Tidal Energy Project (CBTEP) site in Maine, USA. These techniques have proven acceptable to local regulators, the US Department of Energy, the US Federal Energy Regulatory Commission, and the scientific community (Viehman *et al.* 2015). We have incorporated multiple and diverse approaches used in Cobscook Bay to design the mobile survey approach to meet the physical demands of the Minas Passage and the global fish assessment at the site of the turbine. Near-field effects at the device were not the purview of this research.

Material and methods

1. Historical data: 2011-2012

In 2011 and 2012, 6 hydroacoustics mobile surveys (Table 1) were conducted using a split beam echosounder (SIMRAD EK60) operating at 120 kHz using the charter vessel *FUNDY SPRAY* (Melvin and Cochrane 2014). No turbine was present during these surveys. Transmitting power was set at 500W, pulse duration was 1.024 and ping rate at 1/s (to reduce interference with other devices).

Table 1: Summary of the historical dataset surveys conducted in Minas Passage between August 22, 2011 and May 31, 2012.

Survey	Start date	Start time	End date	End time	Day/ Night	Tidal cycle	Number of grids	Water Temperature (°C)	Turbine presence
1	2011-08-22	11:45:18	2011-08-22	21:28:30	D	1	2	15.41	No
2	2011-09-19	10:55:27	2011-09-19	20:22:39	D	1	4	15.7	No
3	2011-11-22	14:22:38	2011-11-22	22:35:59	D/N	1	3	10.3	No
4	2012-01-25	18:32:58	2012-01-25	16:15:18	D/N	2	9	3.57	No
5	2012-03-19	14:23:30	2012-04-19	13:33:06	D/N	2	12	2.5	No
6	2012-05-31	12:09:40	2012-05-31	23:12:16	D/N	1	5	9.51	No

The duration of each survey was either 1 or 2 tidal cycles, as the vessel could only return to port near high tide. The grid for each survey started at the western end of what was the CLA area, and each of the 9 CLA transects was sampled in numerical order, alternating direction (with or

against the current) on each successive 900m transect until arriving at the eastern end of last transect (Figure 1). A transect on the opposite side of the channel (called X1, Figure 2) was then run as the reference transect. An east-to-west transect was sample (Y1) and then a return transect (Y2) ended at the west end of the first transect to finish the first grid (T0; Table 2 and Figure 2).

The EK60 system was calibrated in September 2010 with a 38.1 mm tungsten carbide sphere and calibration settings were applied to all survey data during data processing.

Table 2: Latitude and longitude in decimal degrees used by Melvin and Cochrane (2014) as Minas Channel transects for historic surveys in 2011 and 2012.

Along-Channel	**North-West End**		**South-East End**	
CLA Transect	N	W	N	W
T0	45 22.229	64 26.057	45 22.067	64 25.326
T1	45 22.175	64 26.081	45 22.018	64 25.349
T2	45 22.130	64 26.100	45 21.971	64 25.365
T3	45 22.093	64 26.117	45 21.939	64 25.381
T4	45 22.021	64 26.151	45 21.862	64 25.414
T5	45 21.969	64 26.173	45 21.812	64 25.434
T6	45 21.918	64 26.194	45 21.761	64 25.458
T7	45 21.864	64 26.219	45 21.702	64 25.484
T8	45 21.809	64 26.242	45 21.647	64 25.507
Reference transect	N	W	N	W
X1	45 19.970	64 26.995	45 19.950	64 26.178
Cross- channel transects	N	W	N	W
Y1	45 21.647	64 25.507	45 19.950	64 26.178
Y2	45 22.229	64 26.057	45 19.970	64 26.995

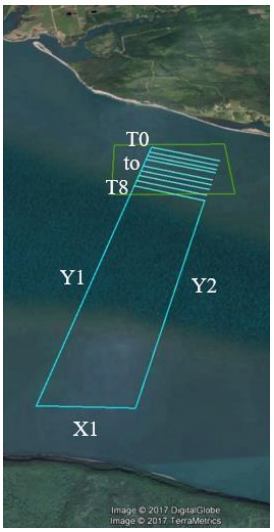

Figure 2: Historic mobile survey design. Collectively, the blue lines show one grid, with transect names indicated by the text. The green square represents the CLA.

Raw data and calibration settings from these 6 historical surveys were provided by Gary Melvin and re-processed using our own data processing methods (see part 4 of Materials and Methods: Data processing).

2. Contemporary data: 2016-2017

The survey design and the echocounder system settings used for historical data collection were used to collect a comparable contemporary dataset. Data were collected with a Simrad EK80 scientific echosounder, mounted over the side of a medium sized boat, the *Nova Endeavor* (Figure 3).

The EK80 is Simrad's newest scientific echosounder system which replaced the previous EK60 system. It has the capability to collect wideband data (spanning a range of frequencies) when operating in frequency modulated (FM) mode. It can also operate at only one frequency, like other scientific echosounders and the EK60, in continuous wave (CW) mode. For the sake of comparison with historical data, the majority of the data collected in 2016 and 2017 were sampled in CW mode at 120 kHz. Only CW data were used in analyses.

Figure 2: The Nova Endeavor at Parrsboro harbor (left) and the mounted echosounder and GPS on the side of the boat (right).

The transducer settings were: pulse duration of 1.024 ms (consistent with historical settings), power of 250W (recommended by Simrad), and ping interval of 250ms (lower than the historical dataset collection settings, which was fixed at 1s to minimize interference with other devices).

Six surveys were performed in 2016 and 2017 (Table 3), with 3 surveys before the turbine deployment (May, August and October 2016) and 3 after turbine deployment (November 2016, January and March 2017).

Table 3: Summary of contemporary surveys conducted in Minas Passage between May 28, 2016 and March 08, 2017. A tidal cycle lasts approximately 12 hours and is composed of two stages: ebb tide and flood tide. A grid consists of one full time through all transects. Generally, two were conducted during the day and two at night.

Survey	Start date	Start time	End date	End time	Day/ Night	# of Tidal cycle	# of grids	Water Tempera-ture (°C)	Turbine presence
1	2016-05-28	06:01	2016-05-29	05:35	D/N	2	4	7	No
2	2016-08-13	09:09	2016-08-14	07:40	D/N	2	4	15	No
3	2016-10-07	05:45	2016-10-08	04:21	D/N	2	4	15	No
4	2016-11-24	08:38	2016-11-25	09:07	D/N	2	4	8.0	Yes
5	2017-01-21	06:55	2017-01-22	05:55	D/N	2	4	1.5	Yes
6	2017-03-21	08:24	2017-03-22	06:04	D/N	2	4	4	Yes

Two calibrations (one for the CW mode and one for the FM mode) were performed before each survey. To calibrate the echosounder, we used the calibration program of the Simrad EK80 echosounder software. One person adjusted the location of the 23mm diameter copper

calibration sphere attached to a monofilament fishing line suspended from a fishing rod in the echosounder beam, while one or two other people looked at the monitor to follow the position of the calibration sphere in the software and communicate to the other person its location in the beam. When the software indicated that adequate beam coverage had been achieved, the RMS Error was automatically calculated and the calibration was considered good if this value was less than 0.2.

The survey design was composed of four grids traversed over 24 hours, which included two tidal cycles (one grid per tidal stage). Every 1.8km transect was performed twice, with and against the tidal current. A grid began at transect N0 (always beginning the first transect with the ebbing tide and conducting it with the current), and each successive transect was traversed in numerical order (N0 to N5). Then a southward across-channel transect (South_CW) terminated near the Passage's southern coastline and was followed by 3 reference transects (S1 to S3), with and against the current. To finish the grid, a northward return transect (North_FM) returned the vessel to N0 and was the only transect performed in frequency modulated mode (Table 4 and Figure 4). A grid consisted of one full time through all transects. Generally, two grids were conducted during the day and two at night.

Table 4: Latitude and longitude in decimal degrees used as Minas Channel transects for contemporary surveys in 2016 and 2017.

	West End		**East End**	
CLA transects:	**Lat**	**Lon**	**Lat**	**Lon**
N0	45.3717	-64.4414	45.3666	-64.4188
N1	45.3701	-64.4424	45. 3648	-64. 4197
N2	45.3684	-64.4435	45.3631	-64.4207
N3	45.3667	-64.4445	45.3613	-64.4216
N4	45.3649	-64.4455	45.3595	-64.4226
N5	45.3717	-64.4414	45.3666	-64.4188
Cross-channel transects:	**Lat**	**Lon**	**Lat**	**Lon**
South_CW	45.3717	-64.4414	45.3352	-64.4605
North_FM	45.3276	-64.4388	45.3717	-64.4414
Reference transects:	**Lat**	**Lon**	**Lat**	**Lon**
S1	45.3352	-64.4605	45.3313	-64.4372
S2	45.3334	-64.4615	45.3296	-64.4380
S3	45.3317	-64.4623	45.3276	-64.4388

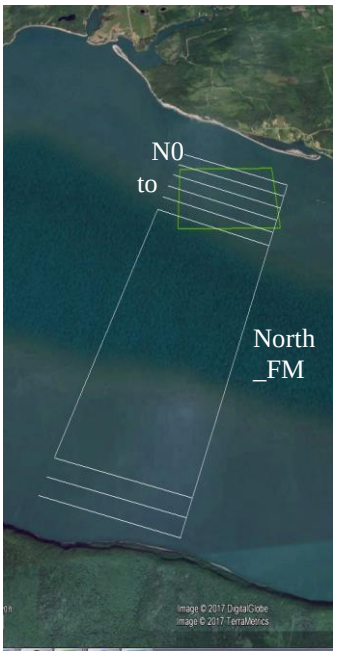

Figure 4: Contemporary survey grid. Thegreen square represents the CLA. White lines show one complete grid, with transects at the- CLA (N0-N5) and reference (S1-S3) sites connected by cross-channel transects (South_CW and North_FM).

3. Data processing

Data processing was performed using the software Echoview® (version 7.1.35; Myriax, Hobart, Australia), which is specialized for the analysis of hydroacoustic data. The data were cleaned (threshold applied and entrained air removed), split into analysis bins, and echo integrated.

A. Threshold

To detect only fish, we used a Target strength (TS) threshold of -60dB and an Sv threshold of -66dB, according the methods from Higginbottom *et al.* (2008). This method allowed us to detect only fish greater than 10cm in length.

B. Entrained air removal

The presence of turbulence and eddies caused large quantities of air to become entrained in the water column, which intermittently contaminated the acoustic data from the surface down to 50 m depth (Figure 5). This impacted the quality of the data on some transects in both the historical and contemporary datasets. During data processing, this entrained air had to be removed so that it would not be echo integrated with the fish.

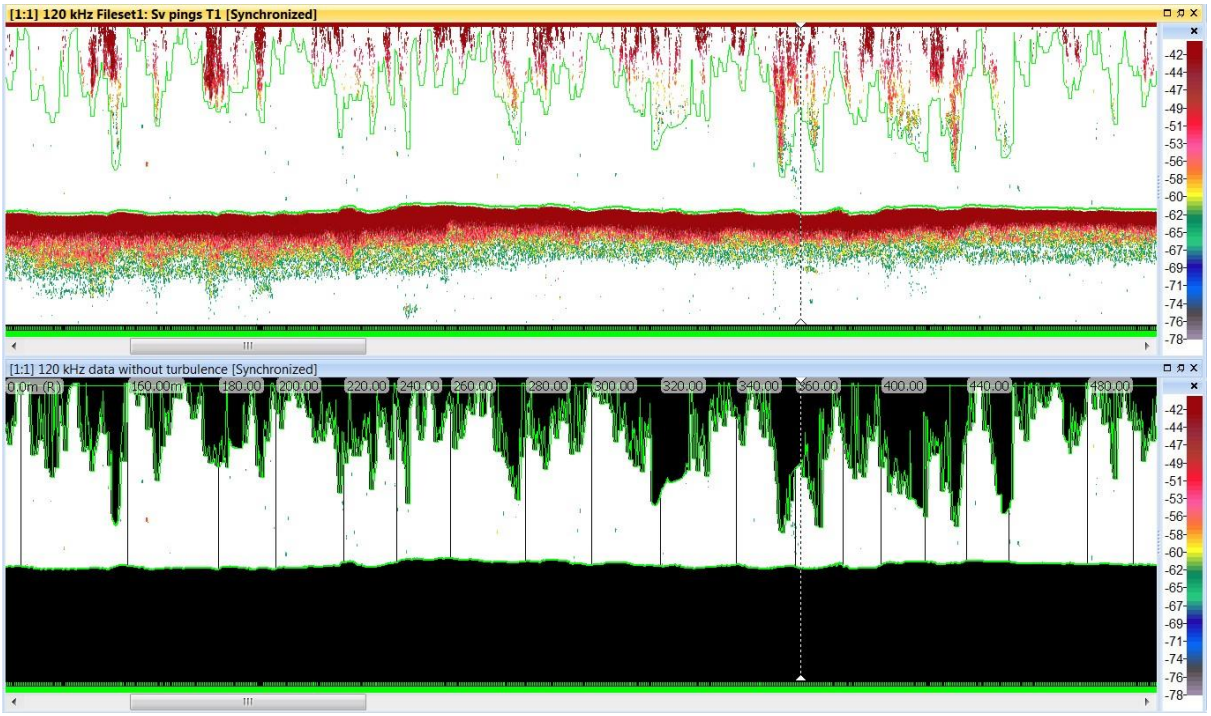

Figure 5: Snapshot of an echogram from October 2016. Top: raw volume backscatter data with target strength threshold of -60dB applied, showing entrained air extending from surface. Bottom: data with entrained air removed, showing turbulence and bottom lines. Data excluded from echo integration indicated by black areas. Vertical lines show 20 m data analysis bins.

To remove entrained air, the raw volume backscatter data were multiplied by -1.0 and a constant was added so Echoview interpreted the surface boundary as the bottom of the water column (Figure 6A). Then, a bottom detection algorithm was applied to the transformed data to identify and smooth the turbulence line—the boundary between entrained air and empty water (Figure 6B). A traditional bottom detection algorithm was applied to untransformed data to detect the actual sea floor (Figure 6C). The data outside the turbulence line and the bottom line were then discarded (Figure 6D), and the data between those two lines were used for echo integration (Figure 6E and Figure 5, bottom).

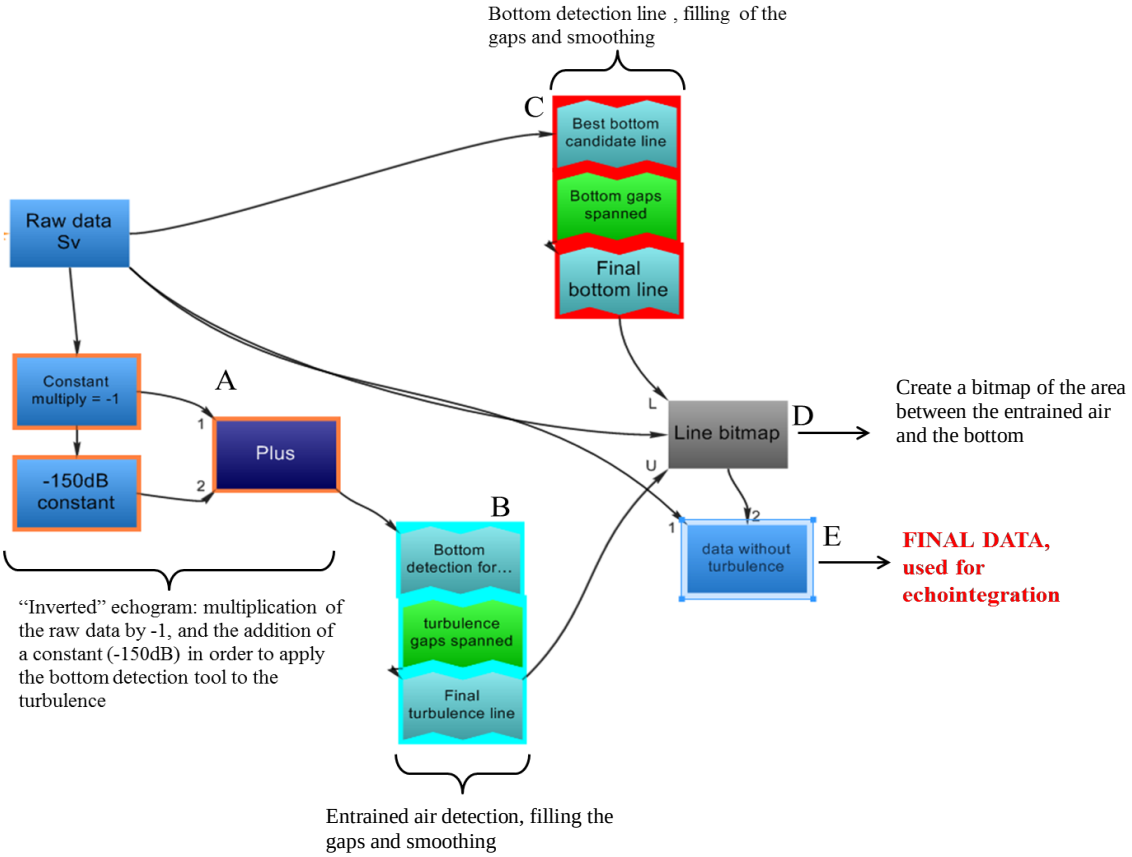

Figure 6: Echoview algorithm for processing data prior to echo integration.

C. Analysis bins: space and time

To assess changes in fish density over time, data were divided into analysis bins spanning the entire water column to provide statistically independent samples. To choose the appropriate bin size to use in echo integration, we performed autocorrelation tests using a range of bin sizes. Bins could either be defined by distance (in meters traveled) or duration (in minutes). We performed autocorrelation tests on 4 randomly chosen transects by grid (GR1_N0A, GR2_N3A, GR3_N5W and GR4_S1W) for each survey. Distance bins were chosen over time bins in order to separate the transects made with or against the tide (since time length differed greatly) in a comparable number of bins based on the distance of a transect. The cleaned acoustic data from each of these transects were partitioned into 5-m distance bins. Each bin was echo integrated, and the resulting volume backscatter values were exported from Echoview and tested for autocorrelation (Figure 7). For the 4 tested transects from all surveys, data became uncorrelated (with a 5% significance level) at 20-m distance bins. As such, all data were split into 20-m distance bins and echo integrated over the entire water column for each transect of each survey (Figure 8, right).

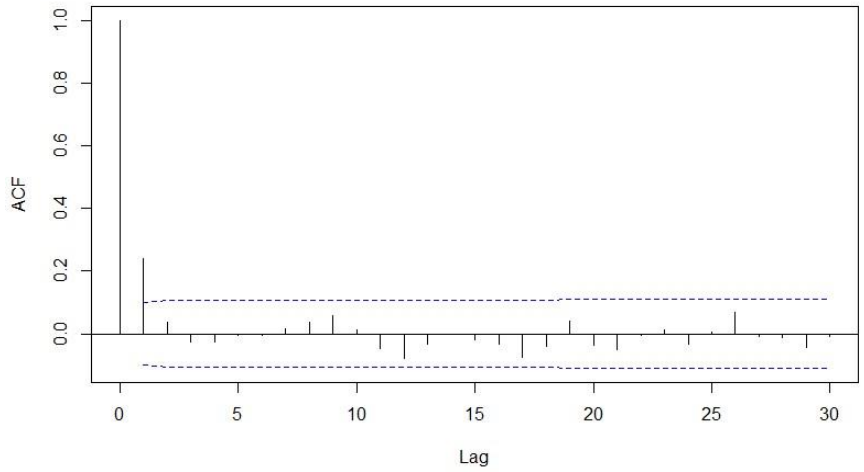

Figure 7: Example of an autocorrelation function (for GR4_S1W). ACF is the autocorrelation function for a given lag, with lag of 1 equivalent to 5 m (the bin size). The dashed blue lines indicate the 95% confidence interval. At lags in which the ACF is within this interval, samples are no longer correlated (e.g., are independent). In this example, samples become independent at lag = 2, or 10 m.

To study fish vertical distribution, the data from each transect were split into depth bins 1 m deep, measured upward from the sea floor (Figure 8, left).

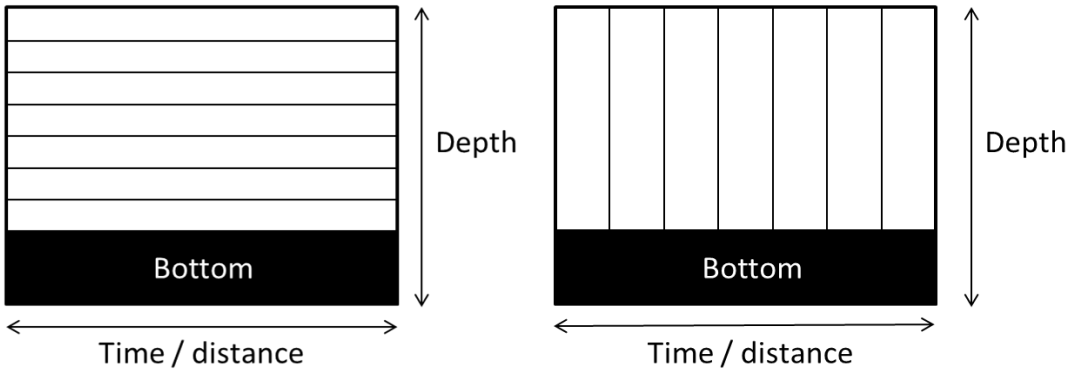

Figure 8: Representation of the data export by 1m depth bins (left) and by 20m vertical distance bins (right).

4. Data Analysis

Data analysis was conducted with the software R (version 1.0.136, R Core Team, Vienna, Austria). We examined changes in water column fish density, the vertical distribution of fish, and the proportion of fish at turbine depth.

A. Water column fish density

To test for indirect effects of the single deployed TISEC device on fish density (throughout the water column), we used the data exported for 20-m distance bins. The data distribution was not normal, with 60.4% of values equal to zero (empty water column). A zero-inflated two-stage generalized linear model (GLM) was created for sv values (volume backscatter in the linear domain, or relative fish density) on the full dataset (historical data and contemporary data combined) to statistically test the effect of site (CLA or reference) and turbine (presence or absence) .

The first stage modeled relative fish density (sv) as a function of fish presence (presence = 0 if sv = 0, or 1 if sv > 0).

***1st stage** = GLM (sv ~ fish presence)*

We then applied the prediction from the first stage to the second stage model and added the variables of interest (site and turbine).

***2nd stage A** = GLM (sv ~ 1st stage + site + turbine)*

To also test for an effect of time of year, we performed another two-stage GLM that incorporated survey month:

***2nd stage B** = GLM (sv ~ 1st stage + site + month)*

B. Fish vertical distribution

To test for indirect effects of a single TISEC device on fish vertical distribution, we worked with the data exported by 1 m depth bins for each individual transect. We calculated the proportion of area backscatter, sa, contributed by each layer (sa for each layer divided by the sa summed for all layers). Depth varied over the course of each transect, between transects, and with the tidal stage (from 40 to 65 meters). As such, we analyzed only the first 50 meters above the bottom.

C. Proportion of fish at turbine depth

To test the probability of fish being at the same depth of the recently deployed bottom-mounted OpenHydro turbine, we used data from the N2 and N3 transects (the two transects closest to the turbine location). We only used data from when the tide was flooding (n=2 for each survey). The turbine was located on the east side of the CLA, so during flood tide, the survey vessel was approaching the turbine. Transect data were echo integrated in three 700 m distance bins (the length of the transect divided by 3), numbered 1 to 3 (1 farthest from the turbine and 3 closest; Figure 9). This allowed us to examine changes in fish density as the boat approached the location of the turbine. Only two transects were conducted directly over the turbine (called 'over-the-turbine transect') when the tide was flooding during the November 2016 survey (Figure 9, left). This over-the-turbine transect was not run again during other surveys because it delayed the timing to complete the surveys planned to quantify indirect mid-field effects.

For each survey, the proportion of fish in the bottom 23 m above the sea floor (turbine height) was calculated for each distance bin at flood tide in N2 and N3 transects.

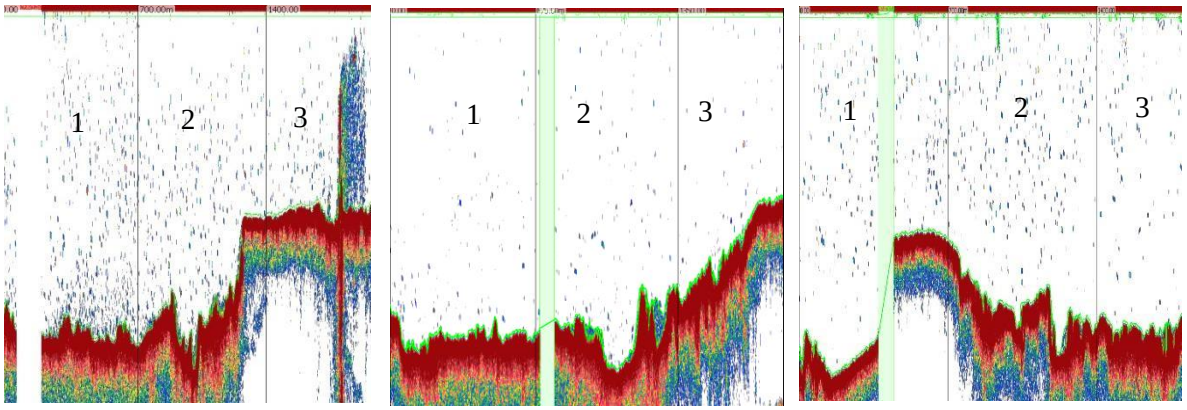

Figure 9: Condensed echograms of flood-tide transects during the November 2016 survey over-the-turbine (left), during the N2 transect (middle), and during the January 2017 survey in N3 transect (right) after entrained air and bottom detection.

The results of these two turbine transects were compared to the results from all N2 and N3 transects conducted in other surveys to determine if N2 and N3 transects (which are 50 m either side of the turbine) reflected the fish distributions at the location of the turbine.

D. Cross-channel distribution

The cross-channel transects were processed to examine the variability in fish distribution across the channel, between the CLA and reference site. Condensed echograms, Sv mean variation and sv boxlot by bins (transect length divided by 3 to obtain one south, one middle and one north bin) were created.

Results and discussion

1. Water column fish density

Changes in fish density were explored as a function of several factors (turbine, survey, month, diel and tide). Boxplots were used to visualize relative fish density (sv) data. All following boxplots show the median fish density (thick horizontal line), interquartile range (colored box), and 10^{th} and 90^{th} percentiles of fish density (whiskers). A large number of 0's (empty water column) resulted in heavily skewed distributions, so non-zero variation is best visualized by the extent of the box and whiskers. The mean or average fish density value is shown by the empty circle in some figures (e.g., Fig. 13), as an indicator of the influence of extreme values (outliers). In all plots, the red color is associated with the CLA site and the blue color with the reference site.

A. Model results

The 2-stage generalized linear model showed a statistically significant effect of survey (month, Pr = 0.037) on fish density, but no significant effect of site or turbine presence (Tables 5 and 6).

Table 5: Results of the two-stage GLM B (factors: fish presence, site and survey month). Df = degrees of freedom, Resid. Df = Residual degrees of freedom, Resid. Dev = Residual Deviance, Pr = probability of observing a Chi square statistic. ** = statistical significance at the p < 0.05 level, * = statistical significance at the p < 0.001 level.**

	Df	Deviance	Resid. Df	Resid. Dev	Pr(>Chi)
Null model			77371	1.9E-07	
Fish presence	1	2.97E-11	77370	1.9E-07	0.0005 ***
Month	5	3.35E-11	77362	1.9E-07	0.037*
Site	1	5.25E-12	77368	1.9E-07	0.34

Table 6: Results of the two-stage GLM A (factors: fish presence, site and turbine).

	Df	Deviance	Resid. Df	Resid. Dev	Pr (>Chi)
Null model			77371	1.9E-07	
Fish presence	1	2.97E-11	77370	1.9E-07	0.0005 ***
Site	1	5.25E-12	77368	1.9E-07	0.34
Turbine	1	7.21E-11	77367	1.9E-07	0.09

The two stage GLM results revealed no significant effect of turbine presence on fish density. However, data are limited and monitoring of the region should continue in order to assess changes in fish distribution patterns over time since seasonal shifts in fish distributions have also been reported in other similar environments (Wilson *et al.*, 2006; Copping *et al.*, 2016; Viehman, 2016). The two stage GLM revealed a statistically significant month effect, where relative densities of fish varied greatly among months in this region, reflecting significant seasonal variability.

B. Fish density before and after turbine deployment

For the full dataset (historic and contemporary data combined), relative fish density (sv) was not statistically significantly different at either site before or after the period when the turbine was present. This is likely based on similar variation in relative fish densities between the sites. However, within sites, fish density upper whisker boxplot was higher at both the CLA and reference sites after the turbine was present (Figure 10). The importance of the reference site is demonstrated by the similarity in changes in fish density at both sites (Figure 10), relative fish density increased ***at both sites*** post deployment. These similarities enable us to not falsely associate these changes with the deployment of the turbine.

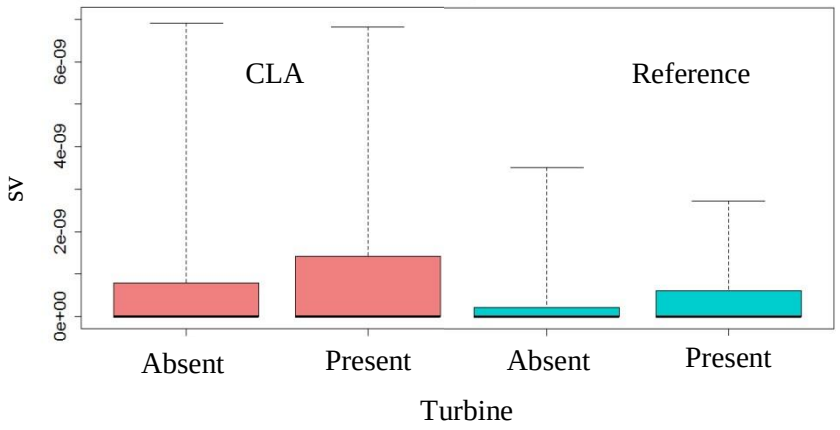

Figure 10: Boxplot of sv (relative fish density) by site before and after turbine deployment (turbine absent or present). Before-deployment data include the historical dataset (2011-2012) and part of the contemporary dataset (May, August, and October 2016); after-deployment data include November 2016 and January and March 2017 of the contemporary dataset.

C. Fish density over time

Fish density was similar among sites but varied by survey timing (Figures 11 and 12). The seasonal variation was similar between historical (2011-2012) and contemporary (2016-2017) data, with consistently higher densities in November and January surveys. This seasonal variation is consistent with the GLM modeling results.

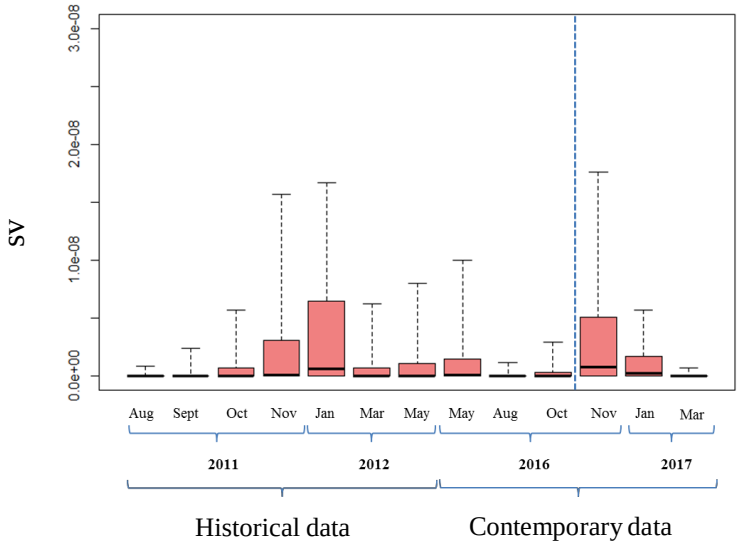

Figure 11: Boxplot of sv (relative fish density) by survey for the CLA site. The dotted blue vertical line indicates turbine deployment.

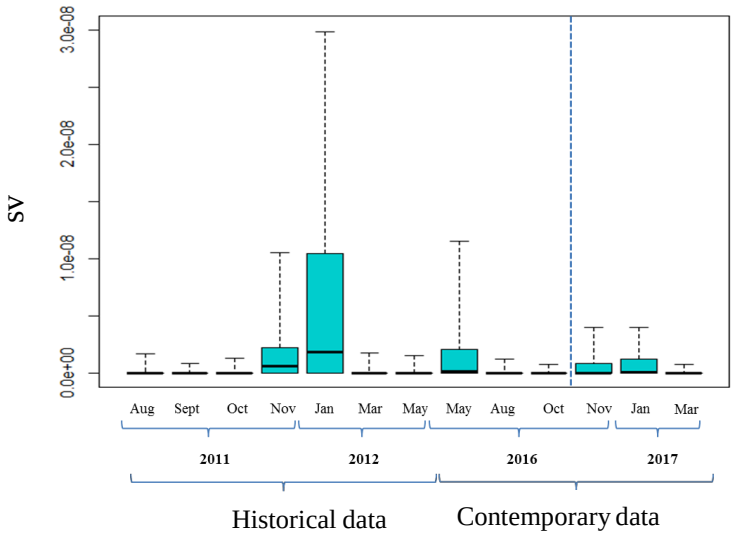

Figure 12: Boxplot of sv (relative fish density) by survey for the reference site. The dotted blue vertical line indicates turbine deployment.

Complementary months of historical and contemporary data showed similar seasonal variation with highest densities in November and January surveys, likely related to specific winter behavior and a higher occupation of the channel in winter. This type of difference was also reported by Keyser *et al.* (2016) for striped bass in Minas Passage.

D. Fish density by month

The contemporary data (Figure 14) had similar interannual relative fish densities as the historical data (Figure 13). Density was high in November and January in both dataset, especially in January 2012 (Figure 13).

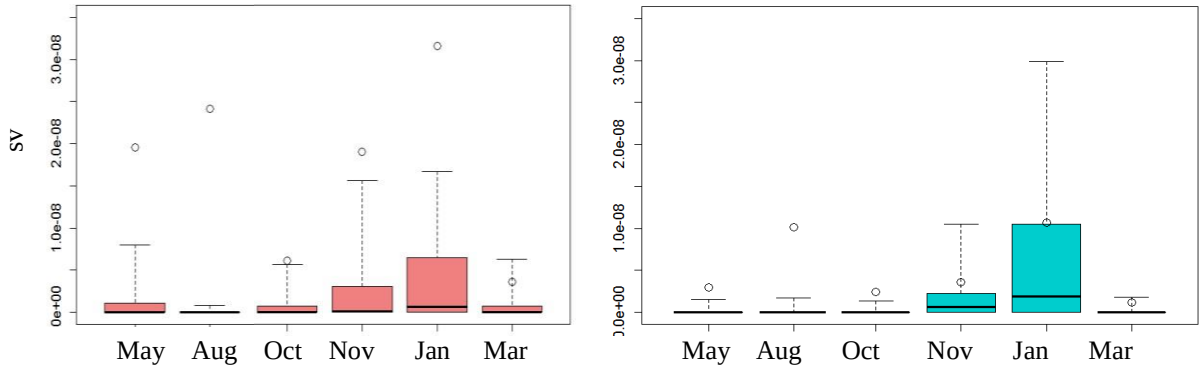

Figure 13: Boxplot of sv (relative fish density) by survey month for historical dataset (2011 and 2012) for CLA site (left, red) and reference site (right, blue).

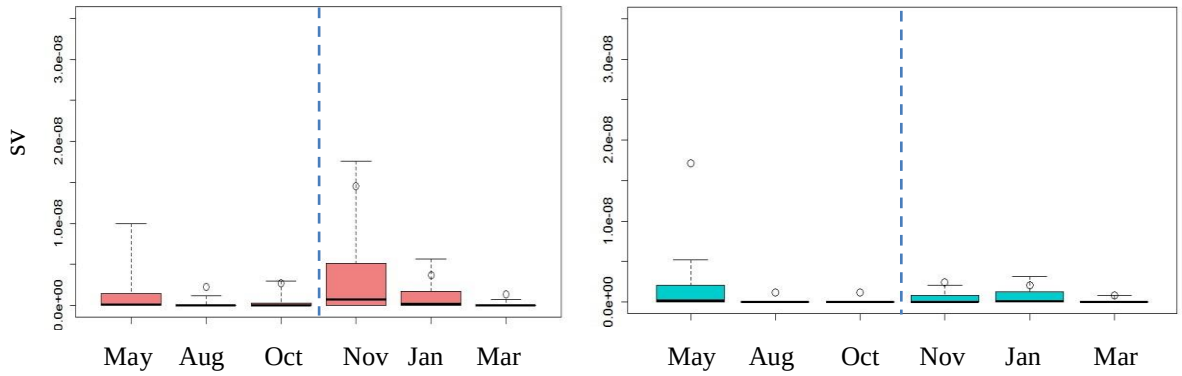

Figure 14: Boxplot of sv (relative fish density) by survey month for contemporary dataset (2016 and 2017) for CLA site (left, red) and reference site (right, blue). The vertical blue line indicates turbine deployment. There is no mean associated with May, CLA site because it was so high that it could not fit into the plot.

High densities in November could be related to emigration of juvenile clupeids. By late fall, young- of- the -year river herring (*Alosa aestivalus*), alewife (*Alosa pseudoharengus*) and Atlantic herring (*Clupea harengus*) are the abundant clupeid species remaining along the northern coast (Ames and Litcher, 2013; Dadswell, 2013). After that period, they are thought to move to deeper, warmer depths through the winter (Townsend *et al.*, 1989), and return to coastal nurseries in the spring.

Higher fish density in May (especially in 2016) was observed. This may have been associated with adult alewife spring spawning migrations and the presence of Atlantic herring and striped bass (*Morone saxatilus*) (Baker et *al.*, 2014). Striped bass are common in the Minas Passage along the shoreline and they spawn in the head of the tide in May-June (Rulifson and Dadswell, 1995). Spring variation may also be linked to other species migrating into the Basin for the summer, e.g. Atlantic sturgeon (*Acipenser oxyrhynchus*), American shad (*Alosa sapidissima*), American mackerel *(Scomber scombrus*), and rainbow smelt (*Osmerus mordax*) (Dadswell 2010).

E. Fish density by tide and by diel stage

Overall (historical data and contemporary data combined), relative fish density (sv) was similar during ebb and flood tides. However, mean fish density (the unfilled circles on Figure 15) was higher during ebb tides than during flood tides, reflecting a higher number of extreme values (outliers), perhaps indicating movement of big fish or aggregations of fish into the basin with the ebb tide (Figure 15).

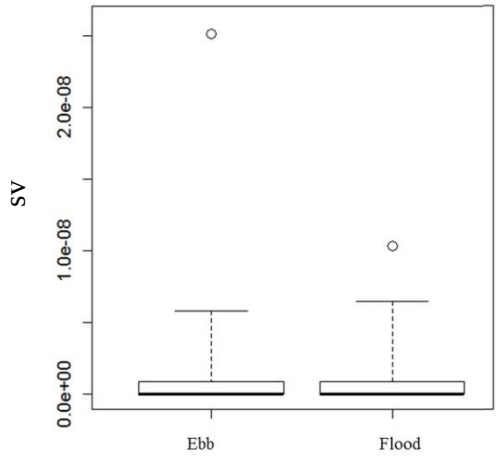

Figure 15: Boxplot of sv (relative fish density) by tidal stage for historical and contemporary data combined.

For all data examined, fish density was similar day and night with higher variability at night than during the day (Figure 16, left). Mean relative fish density during the day was higher than during the night for historical data (2011-2012) while the opposite was observed in the contemporary data (2016 -2017; Figure 16, right).

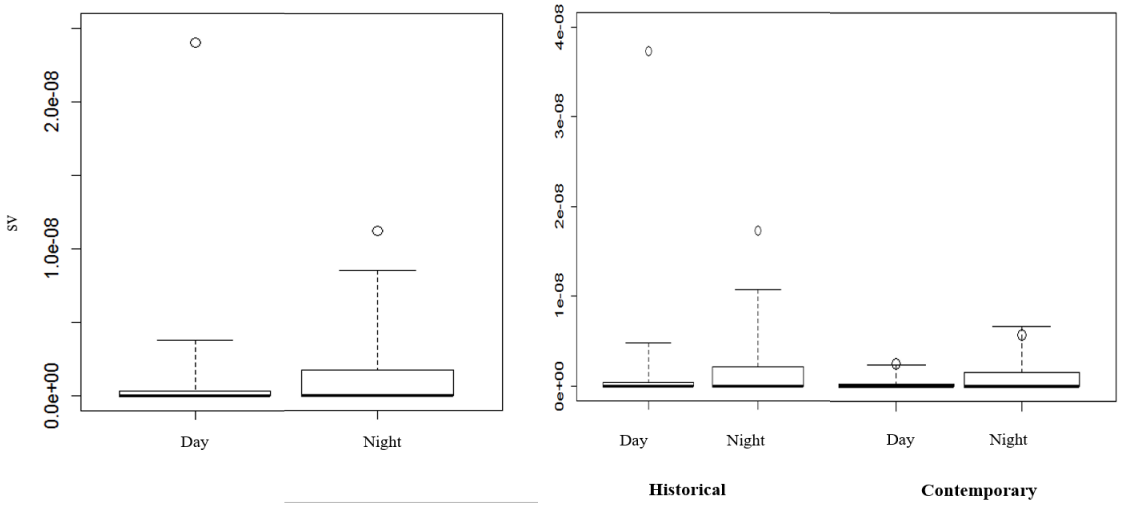

Figure 16: Boxplot of sv (relative fish density) by diel stage for all the data (left), historical (2011-2012) and contemporary data (2016-2017) separated (right). Mean data are shown by the unfilled circles.

In the historical dataset, the higher mean relative fish densities observed during the day may be explained by the numerous outliers, particularly since the highest probability of observing fish aggregations occurs during the day and more samples were collected during the day during the historical surveys. Also, some fish aggregate during the day and tend to spread out more at night (Viehman, 2016), perhaps this diel dynamic can be explained by these changing behaviors.

It is well known that fish densities are generally higher at night at similar tidal energy sites (e.g., Cobscook Bay, ME; Viehman *et al.* 2015; Viehman and Zydlewski, 2017) and with up-looking stationary hydroacoustic surveys in the FORCE site (Viehman, personal

communication). Furthermore, ebb tide sampling showed higher relative fish densities. Thus, fish behavior has been inferred to result in different densities being observed during different tidal and diel stages (Helfman, 1993; Viehman and Zydlewski, 2017).

G. Cross-channel distribution

Cross-channel transects were explored to visualize the distribution of fish across Minas Passage (from the CLA to the reference site). We selected the May 2016 and January 2017 surveys to demonstrate the variation in fish density across the channel (Figure 16). Visualizations of other cross-channel surveys can be found in Appendix I.

Fish density varied along the channel cross-section (Appendix I) and tended to increase south toward the reference site in Figure 16. In these examples, fish density on the CLA side was more variable than on the reference site (south) side of the Minas Passage. The middle part of the Passage, despite its deeper depth (120 meters), did not have higher fish density. Nevertheless, there was high variability in cross-channel distribution (Appendix I) and patterns across the channel cannot be generalized using this dataset.

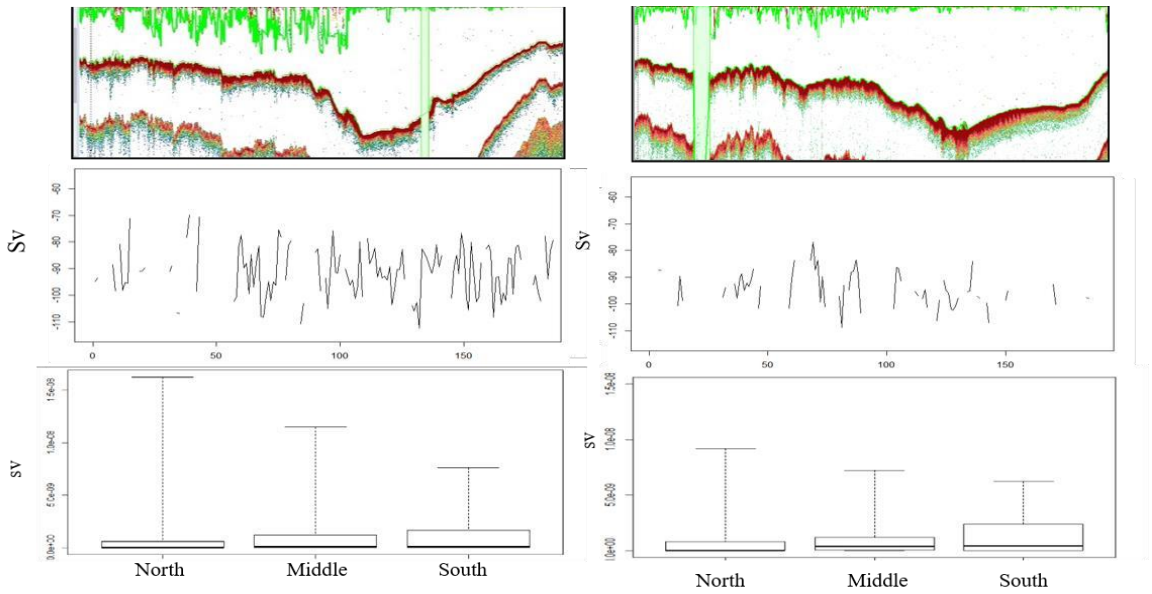

Figure 16: January 2017 survey, flood tide (left) and May 2016 survey, flood tide (right). Condensed echogram of cross-channel transects (top), mean relative fish density (middle) and boxplot of fish relative density (bottom). In the condensed echograms, the beginning (left side) is the CLA and the end (right side) is the arrival at the reference site. There is a double bottom and the green vertical bars are passive data that have not been echo-integrated. In the mean relative fish density (Sv) plot, the x-axis is distance in 20m bins. In the relative fish density boxplot (sv), the relative fish density is plotted in 3 bins (North, Middle and South) to separate the cross-channel into 3 equal distance bins.

2. Fish Vertical Distribution

Relative fish densities in vertical bins of the water column varied among month and between CLA and reference sites (Figure 17).

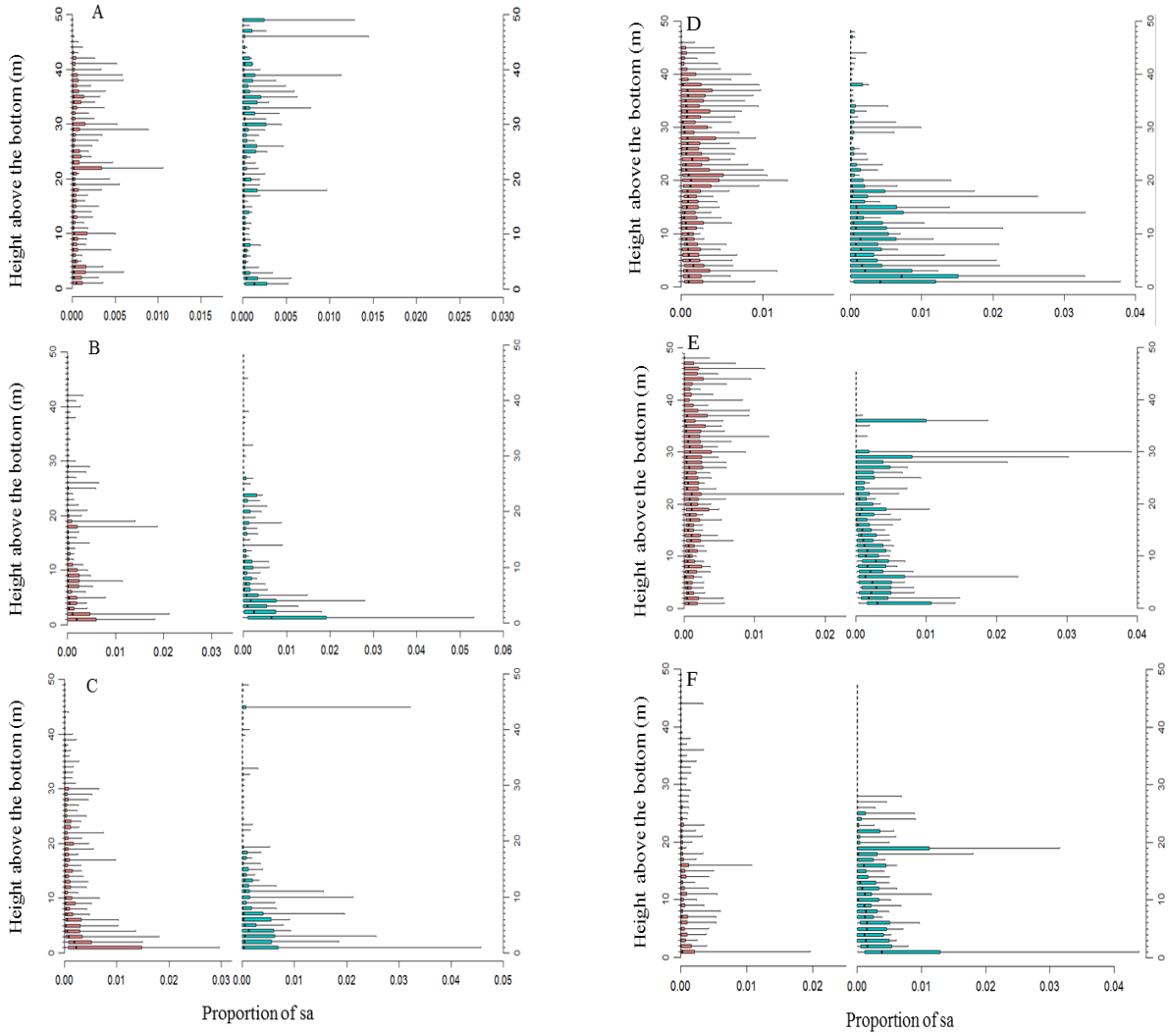

Figure 17: Boxplot of proportion of backscatter (sa, relative fish density) before the turbine deployment by layer for May (A), August (B), October (C), November (D) 2016, January (E) and March (F) 2017, by site (CLA in red, left and reference in blue, right). The proportion of sa (x axis) is very small because numerous outliers have not been plotted so that trends in vertical distributions can be observed.

Fish vertical distributions were highly variable within month and sites. Nevertheless, in August and November, the fish were more concentrated in the first 10 meters above the bottom. These densities could be related to benthic-oriented fish presence. Numerous demersal species occupy the channel, e.g., Atlantic sturgeon (*Acipenser oxyrinchus*), brook trout (*Salvelinus fontinalis*), wolffish (*Anarhichas lupus*), sea raven (*Hemitripterus americanus*), grubby (*Myoxocephalus aeneus*), etc and can contribute to this higher bottom density concentration (Dadswell, 2013). In most other months fish were more evenly distributed throughout the water column and could be various pelagic species mentioned previously, including clupeids.

3. Proportion of fish at turbine depth

The proportion of fish at the depth of the turbine in the spatial bin associated with the turbine (23 m above the sea floor), at a location adjacent to the turbine, was overall lower than the proportion of fish at the same depths in the spatial bins away from the turbine location; distance bins 1 and 2 in Figure 9; Table 7). The proportion of fish at the depth of the turbine in the distance bin nearest the turbine varied among surveys, with a minimum of 1.77% in August 2016 and a maximum of 51.35% in November 2016.

Figure 18 shows the proportion of fish at the depth of the turbine for adjacent N2 and N3 transects with a global lower proportion in the interval 3 where the turbine is/will be located. Figure 19 showed an increasing proportion of fish while we approached the turbine during the Over-the-turbine transect. Taken together, the proportion of fish at the depth of the turbine (Figure 19) during the transect Over-the-turbine was drastically different from the proportions observed in the adjacent N2 and N3 transects (Figure 18).

Table 7: Summary of the percentage of sv (relative fish density) at the turbine depth for each survey and distance bin. Bin 1 is farthest from the turbine location, while bin 3 (in red) is closest. The depth of each interval is also given with the transect depth range. Percent of sv in each bin is also shown for the transect conducted over-the-turbine in November 2016.

Survey	Transect depth range	Interval	Proportion of fish at the depth of the turbine at adjacent transects (see Figure 18)	Proportion of fish at the depth of the tubine in the over-the-turbine transect (see Figure 19)
May-16	45m	1	93.23	
May-16	40m	2	44.81	
May-16	30m	3	**20.48**	
Aug-16	45m	1	23.68	
Aug-16	40m	2	67.09	
Aug-16	30m	3	**1.77**	
Oct-16	45m	1	97.42	
Oct-16	40m	2	29.63	
Oct-16	30m	3	**38.73**	
Nov-16	45m	1	57.11	**21.60299**
Nov-16	40m	2	52.24	**46.50778**
Nov-16	30m	3	**51.35**	**78.07587**
Jan-17	45m	1	71.17	
Jan-17	40m	2	80.39	
Jan-17	30m	3	**3.3**	
Mar-17	45m	1	54.79	
Mar-17	40m	2	32.69	
Mar-17	30m	3	**32.24**	

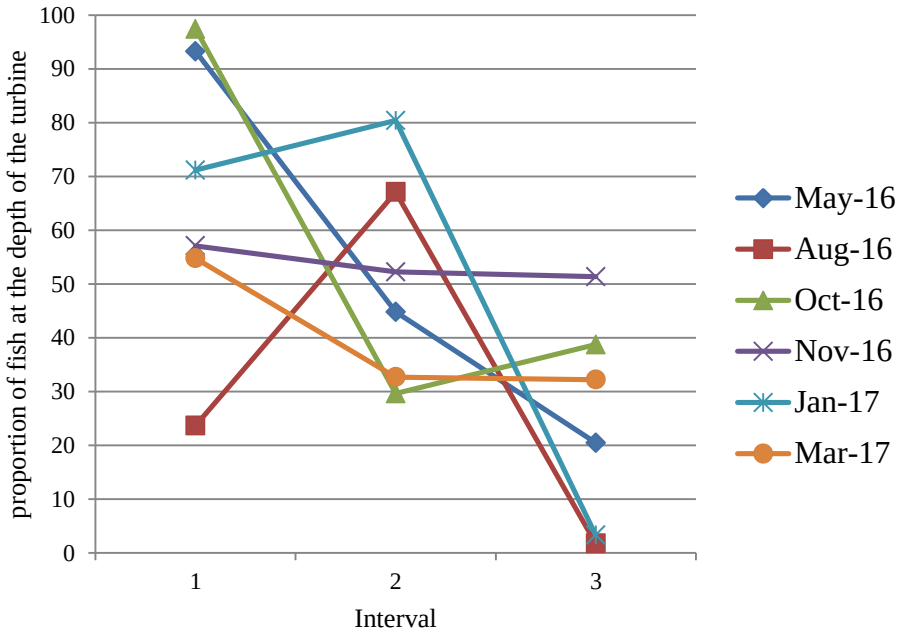

Figure 18: Percent of backscatter (relative fish density, sv) at the depth of the turbine by interval and survey. This plot only includes data from the two transects adjacent to the turbine (N2 and N3).

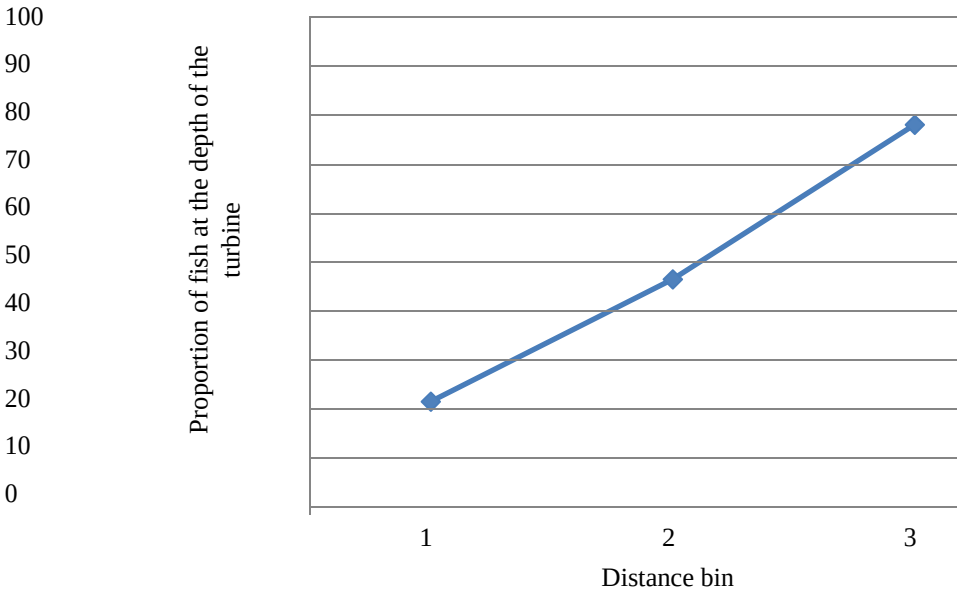

Figure 19: Percent of backscatter (relative fish density, sv) at the depth of the turbine by interval for the transect conducted over-the-turbine in November 2016.

The proportion of fish observed at the same depth of the turbine for the adjacent transects in November were not similar to the over-the-turbine transect. As such, the adjacent transects do not offer a good representation of the fish vertical distribution over a turbine. Therefore, conducting additional surveys repeatedly over-the-turbine would be necessary to assess near-field fish behavioral avoidance (or evasion) when approaching the turbine and developing a full probability of encounter model as in Shen *et al* (2016).

Summary and Conclusions

Six fish surveys were successfully conducted by UMaine and FORCE staff in 2016 and 2017. During these surveys, the FORCE staff was trained to conduct mobile surveys to collect quality data for comparative processing and analysis. The data collected were fully calibrated, making it reliable and comparable among samples. The data were good quality, despite the presence of entrained air at the surface since the entrained air was not integrated into the dataset. Data processing was efficient and allowed the removal of entrained air, export of relative fish density metrics, and comparisons within and between contemporary and historic surveys. Statistical analyses were limited to a two stage GLM because of the non-normality of the data. Additional analyses could focus on the use of an index or way to "normalize" the data but that is beyond the scope of this report.

Conclusions related to the originally stated study objectives:

Objectives 1 and 2: *testing for indirect effects of TISEC devices on (1) relative fish density throughout the entire water column*; and (2) *fish vertical distributions*

- While statistical tests revealed no significant effect of turbine presence on fish density, data are limited to 9 surveys before the deployment and 3 after the deployment. As such, monitoring should continue in order to assess changes in fish distribution patterns as the site is further developed.
- High variability was observed within surveys and among surveys for fish density and vertical distribution. This supports the conclusion that assessment of fish distribution should continue. Trends detected included higher fish densities at night and during ebb tides with seasonal variation being high but fish densities generally highest in May, November and January. Because these patterns are consistent with fish distribution patterns reported in the literature, this type of data collection and analysis suggests the approach can be used to document such patterns.

Objective (3) *estimating the probability of fish being at the same depth of the turbine based on the vertical distribution of fish relative to a deployed TISEC device depth.*

- The proportion of fish at the turbine depth varied greatly.
- As such, a full probability of encounter model could not be developed with the data as collected.

Recommendations

- A valid approach to monitoring the regional responses to changes in the CLA has been developed and should be used moving forward.
- Monitoring should continue in order to assess changes in fish distribution patterns as the site is further developed.
- To keep the data quality high, continue to choose the day of the survey by using the tide calendar, choose a less than 9m difference between high tide level and low tide level and keep the boat running at 5-6knots, no more (unless in the transect is going with the tide when the current is too fast).
- Ideally, physical sampling of fish should be conducted to verify the presence of species seasonally.
- To develop a complete probability of encounter model additional transects over-the-turbine should be conducted.

References

Ames, E., and Lichter, J. (2013). Gadids and alewives: structure within complexity in the Gulf of Maine. *Fisheries Research*, 141, 70-78.

Baker, M., Reed, M., and Redden, A. (2014). "Temporal Patterns in Minas Basin Intertidal Weir Fish Catches and Presence of Harbour Porpoise during April – August 2013." ACER, Wolfville, NS, Tech. Rep. 120.

Copping, A., Sather, N., Hanna, L., Whiting, J., Zydlewski, G., Staines, G., Gill, A., Hutchison, I., O'Hagan, A., Simas, T., Bald, J., Sparling C., Wood, J., and Masden, E. (2016. Annex IV 2016 State of the Science Report: Environmental Effects of Marine Renewable Energy Development Around the World.

Dadswell, M. (2010). Occurrence and migration of fishes in minas passage and their potential for tidal turbine interaction.

Helfman, G. (1993) Fish behaviour by day, night, and twilight. *In*: Pitcher, T.J. (ed.), *Behaviour of Teleost Fishes*, 2nd edn. Chapman and Hall, London, pp. 479-512.

Higginbottom, I., Woon, S. & Schneider, P. (2008). Hydroacoustic data processing for standard stock assessment using Echoview: technical manual.

Keyser, F., Broome, J., Bradford, R., Sanderson, B., & Redden, A. (2016). Winter presence and temperature-related diel vertical migration of striped bass (Morone saxatilis) in an extreme high-flow passage in the inner Bay of Fundy. Canadian Journal of Fisheries and Aquatic Sciences, 73(12), 1777-1786.

McLennan, D., & Simmonds, E. (2013). Fisheries acoustics (Vol. 5). Springer Science & Business Media.

McLean, M., Simpfendorfer, C., Heupel, M., Dadswell, M. & Stokesbury, M. (2014). Diversity of behavioural patterns displayed by a summer feeding aggregation of Atlantic sturgeon in the intertidal region of Minas Basin, Bay of Fundy, Canada. Marine Ecology Progress Series, 496, 59-69.

Melvin, G. and Cochrane, N. (2014). Investigation of the vertical distribution, movement and abundance of fish in the vicinity of proposed tidal power energy conversion devices. Final Report submitted to Offshore Energy Research Association (OERA), Research Project 300-170-09-12. December.

Rulifson, R., & Dadswell, M. (1995). Life history and population characteristics of striped bass in Atlantic Canada. Transactions of the American Fisheries Society, 124(4), 477-507.

Scott, J. (1988). Seasonal spatial distribution of groundfish of the Scotian Shelf and the Bay of Fundy 1974 -79 and 1980-84. Can. Tech. Rep. Fish. Aquat. Sci. 1853.

Shen, H., Zydlewski, G., Viehman, H, & Staines, G. (2016). Estimating the probability of fish encountering a marine hydrokinetic device. Renewable Energy, 97, 746-756.

Stokesbury, M., Logan-Chesney, L., McLean, M., Buhariwalla, C., Redden, A., Beardsall, J. & Dadswell, M. (2016). Atlantic sturgeon spatial and temporal distribution in Minas Passage, Nova Scotia, Canada, a region of future tidal energy extraction. PLoS One, 11(7), e0158387.

Townsend, D., Radtke, R., Morrison, M., Folsom, S. (1989). Recruitment implications of larval herring overwintering distributions in the Gulf of Maine, inferred using a new otolith technique. Marine Ecolocial Progress Series. 55, 1–13.

Viehman, H. & Zydlewski, G. (2015). Fish interactions with a commercial-scale tidal energy device in the natural environment. Estuaries and Coasts, 38(1), 241-252.

Viehman, H. (2016). Hydroacoustic Analysis of the Effects of a Tidal Power Turbine on Fishes. Doctoral Dissertation. University of Maine.

Viehman, H., & Zydlewski, G. (2017). Multi-scale temporal patterns in fish presence in a high-velocity tidal channel. PloS one, 12(5), e0176405.

Wilson, B., Batty, R., Daunt, F. & Carter, C. (2006). Collision risks between marine renewable energy devices and mammals, fish and diving birds: Report to the Scottish Executive.

Appendix I

Condensed echogram from cross channel transects (from the CLA to the reference site) are presented for all surveys (top of the plots). They are associated to mean relative fish density, Sv plots echo integrated by 20m distance bins (middle of the plots) and boxplot of fish relative density, sv (bottom of the plots) to assess the fish density variation along the channel (separated into 3 interval: North, middle, south).

A double bottom echo can be present in the condensed echogram and the green vertical bar is passive data that we collected but which are not echo-integrated.

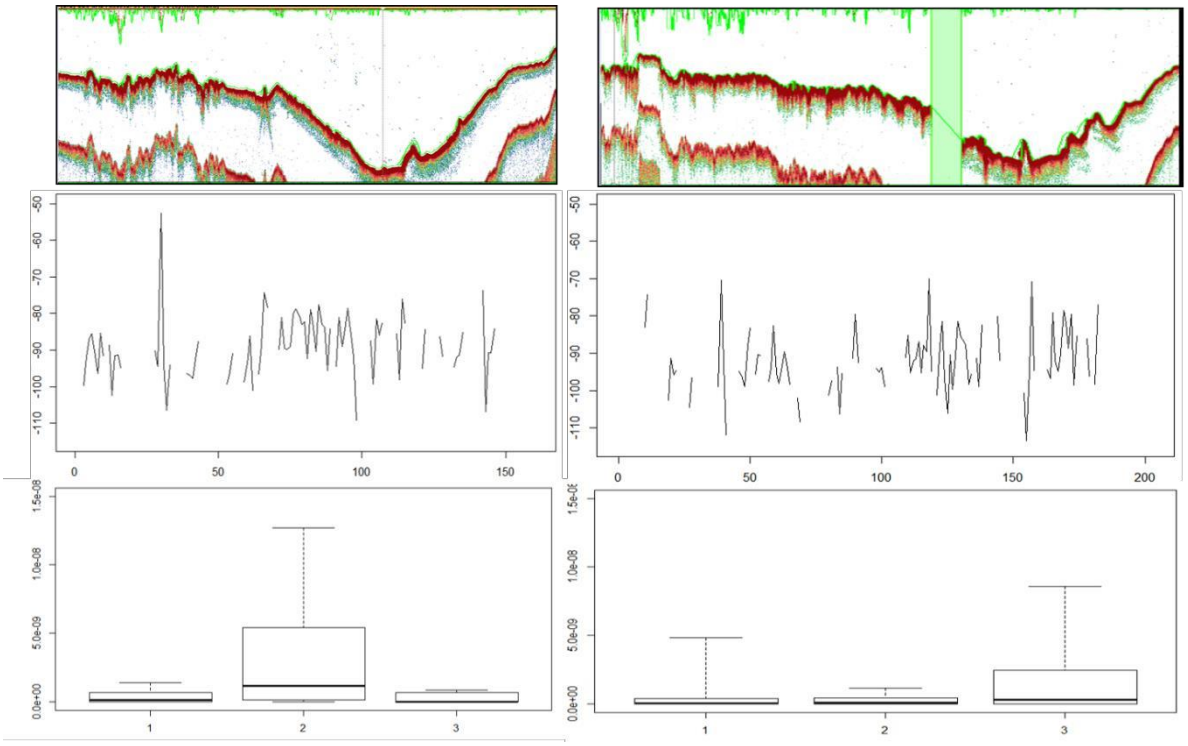

Figure A1: May survey, ebb tide grid 1 (left) and ebb tide grid 3 (right). Condensed echogram of cross-channel transects (top), mean relative fish density (middle) and boxplot of fish relative density (bottom).

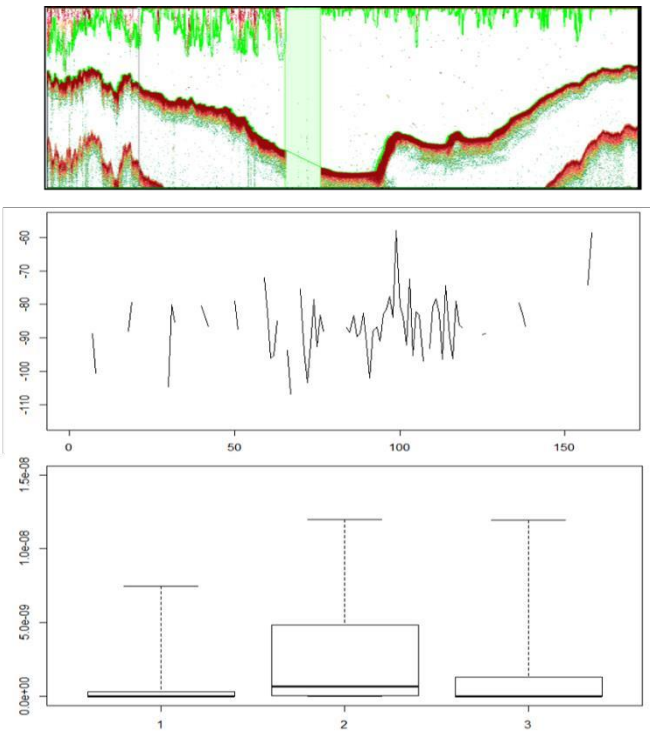

Figure A2: May survey, flood tide grid 4. Condensed echogram of cross-channel transect (top), mean relative fish density (middle) and boxplot of fish relative density (bottom). The May flood tide grid 2 is presented in Figure 16 (right).

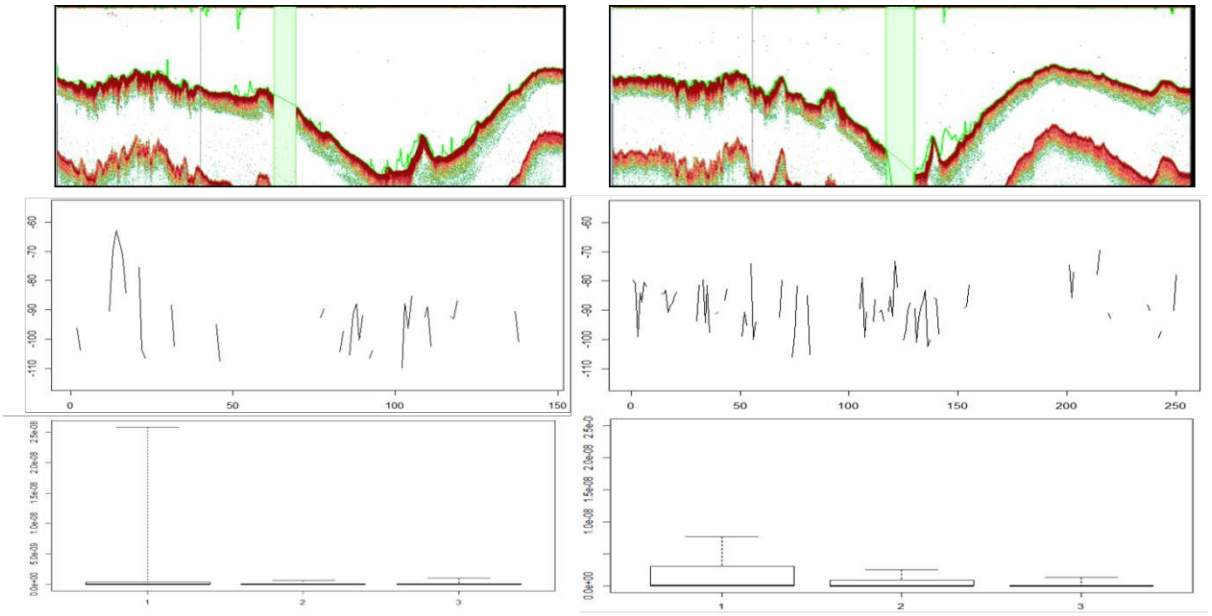

Figure A3: August survey, ebb tide grid 1 (left) and ebb tide grid 3 (right). Condensed echogram of cross-channel transects (top), mean relative fish density (middle) and boxplot of fish relative density (bottom).

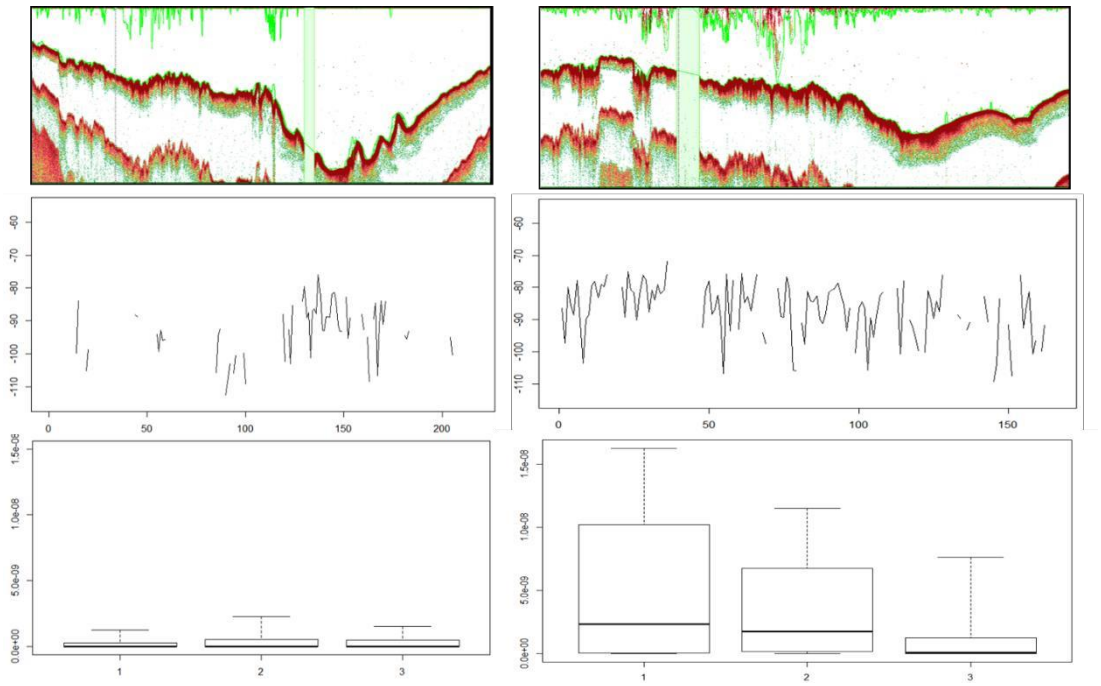

Figure A4: August survey, flood tide grid 2 (left) and flood tide grid 4 (right). Condensed echogram of cross-channel transects (top), mean relative fish density (middle) and boxplot of fish relative density (bottom).

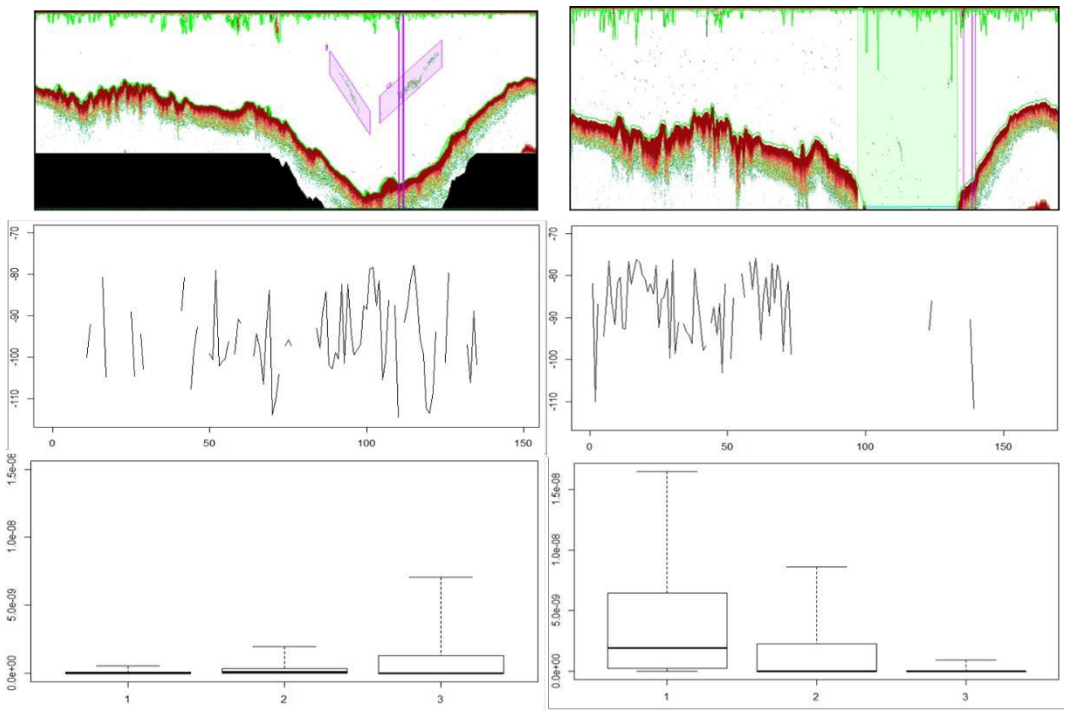

Figure A5: October survey, ebb tide grid 1 (left) and ebb tide grid 3 (right). Condensed echogram of cross-channel transects (top), mean relative fish density (middle) and boxplot of fish relative density (bottom). The purple vertical bars and area correspond to bad data and have not been echointegrated.

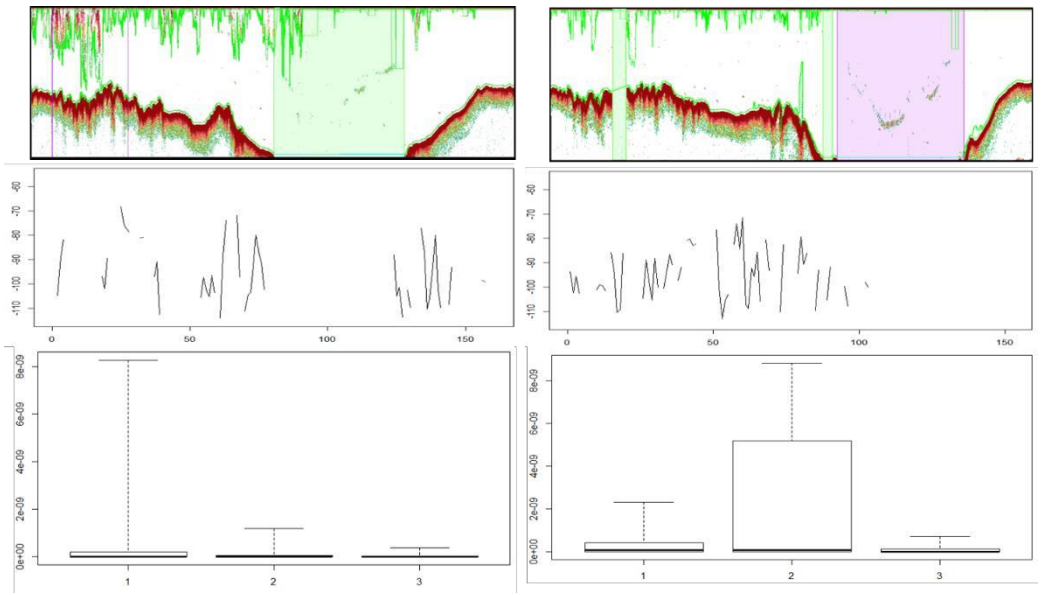

Figure A6: October survey, flood tide grid 2 (left) and food tide grid 4 (right). Condensed echogram of cross-channel transects (top), mean relative fish density (middle) and boxplot of fish relative density (bottom). The purple vertical bars and area correspond to bad data and have not been echointegrated.

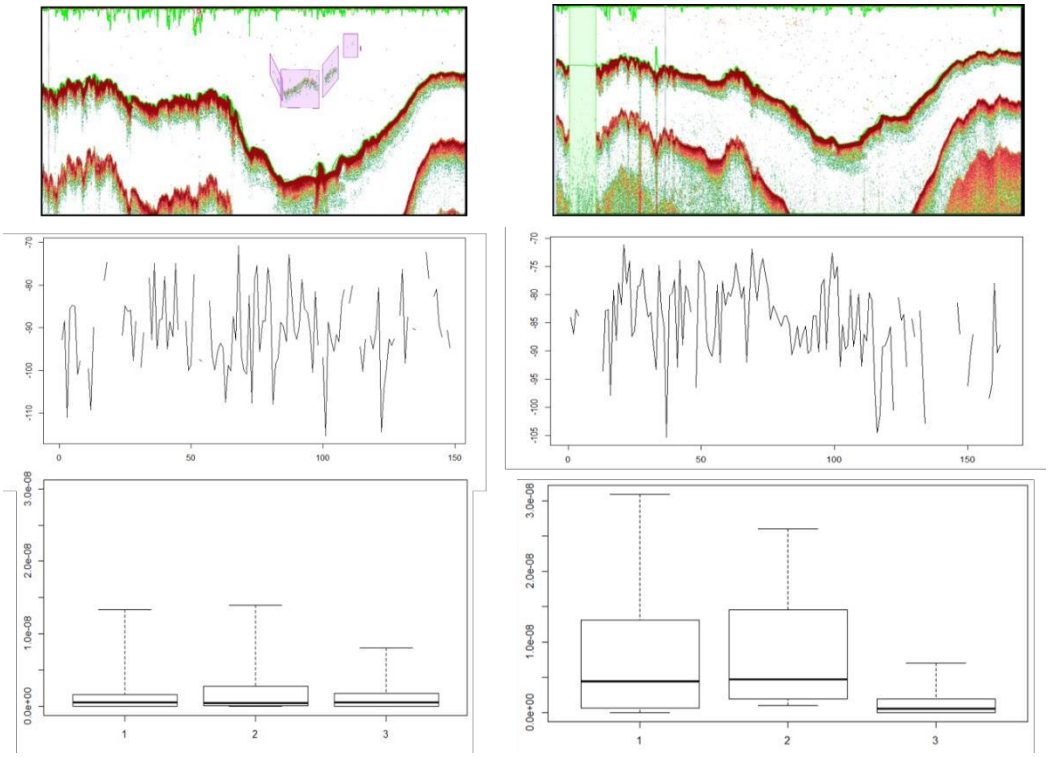

Figure A7: November survey, ebb tide grid 1 (left) and ebb tide grid 3 (right). Condensed echogram of cross-channel transects (top), mean relative fish density (middle) and boxplot of fish relative density (bottom). The purple vertical bars and area correspond to bad data and have not been echointegrated.

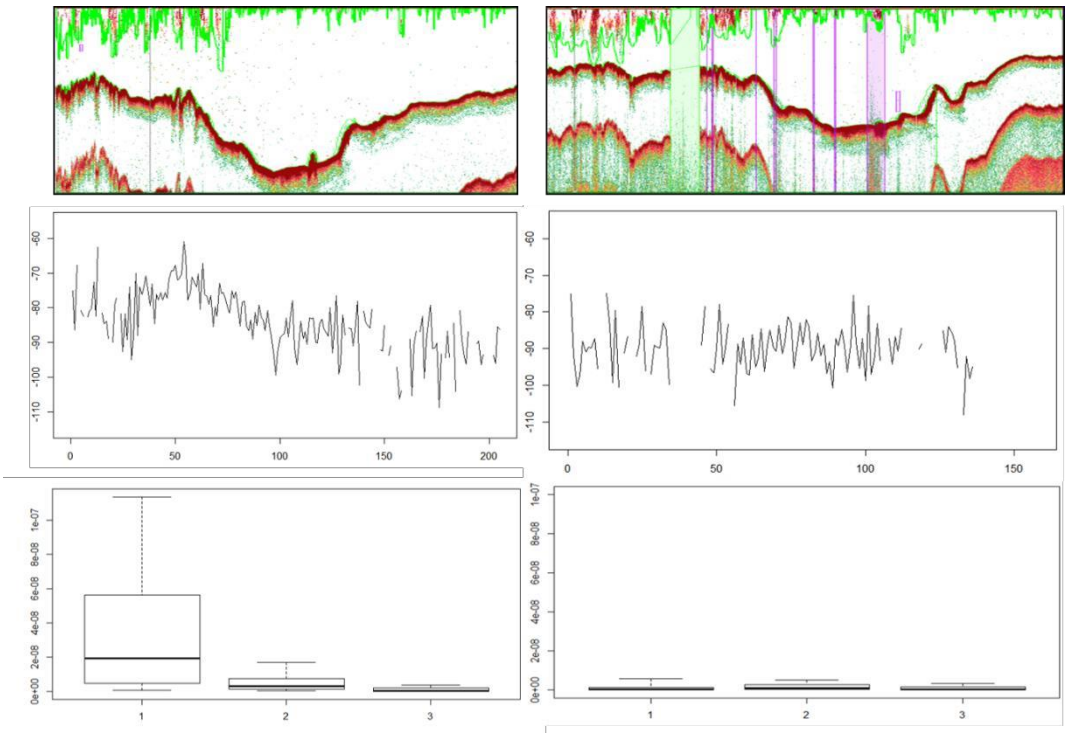

Figure A8: November survey, food tide grid 2 (left) and flood tide grid 4 (right). Condensed echogram of cross-channel transects (top), mean relative fish density (middle) and boxplot of fish relative density (bottom). The purple vertical bars and area correspond to bad data and have not been echointegrated.

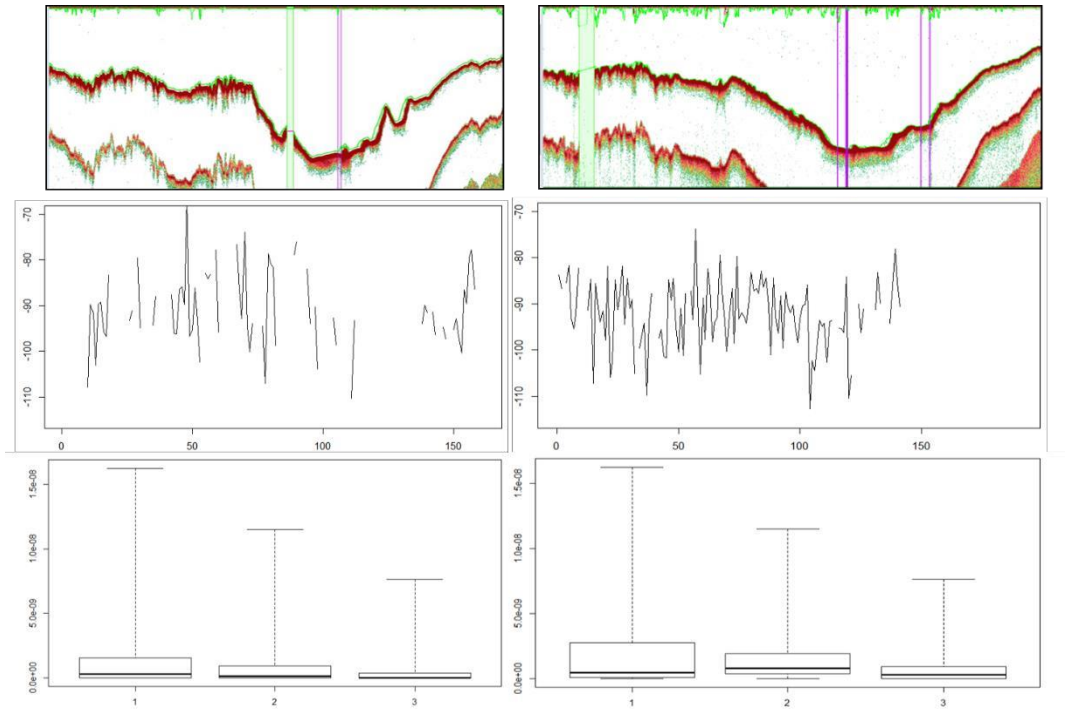

Figure A9: January survey, ebb tide grid 1 (left) and ebb tide grid 3 (right). Condensed echogram of cross-channel transects (top), mean relative fish density (middle) and boxplot of fish relative density (bottom). The purple vertical bars and area correspond to bad data and have not been echointegrated.

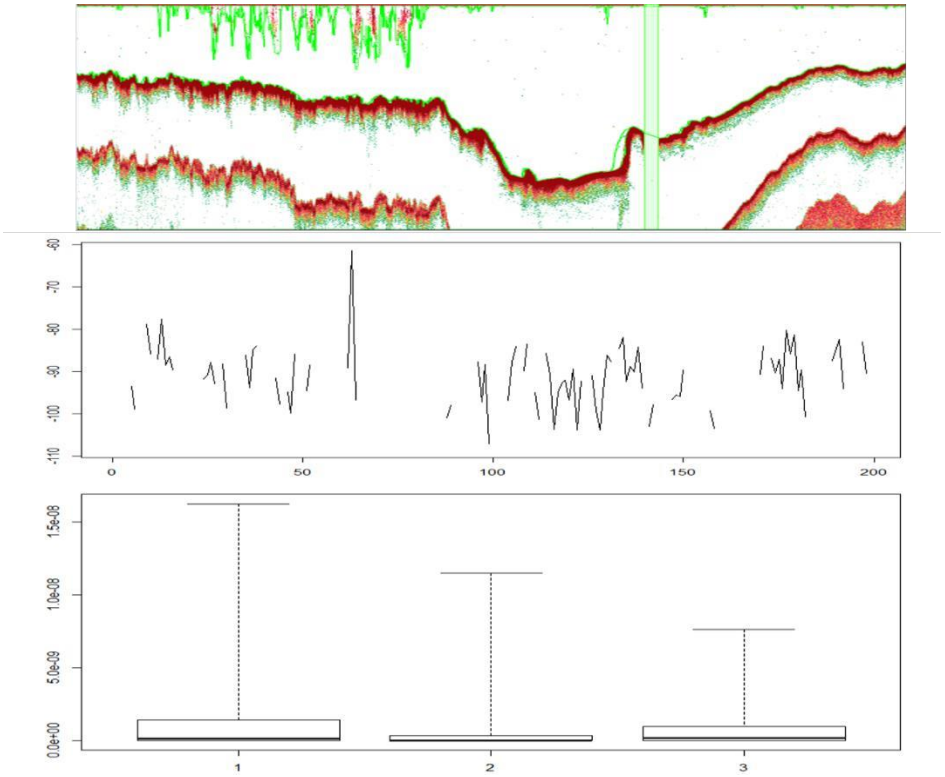

Figure A10: January survey, food tide grid 4. Condensed echogram of cross-channel transect (top), mean relative fish density (middle) and boxplot of fish relative density (bottom). The January flood tide grid 2 is represented in Figure 16 (left).

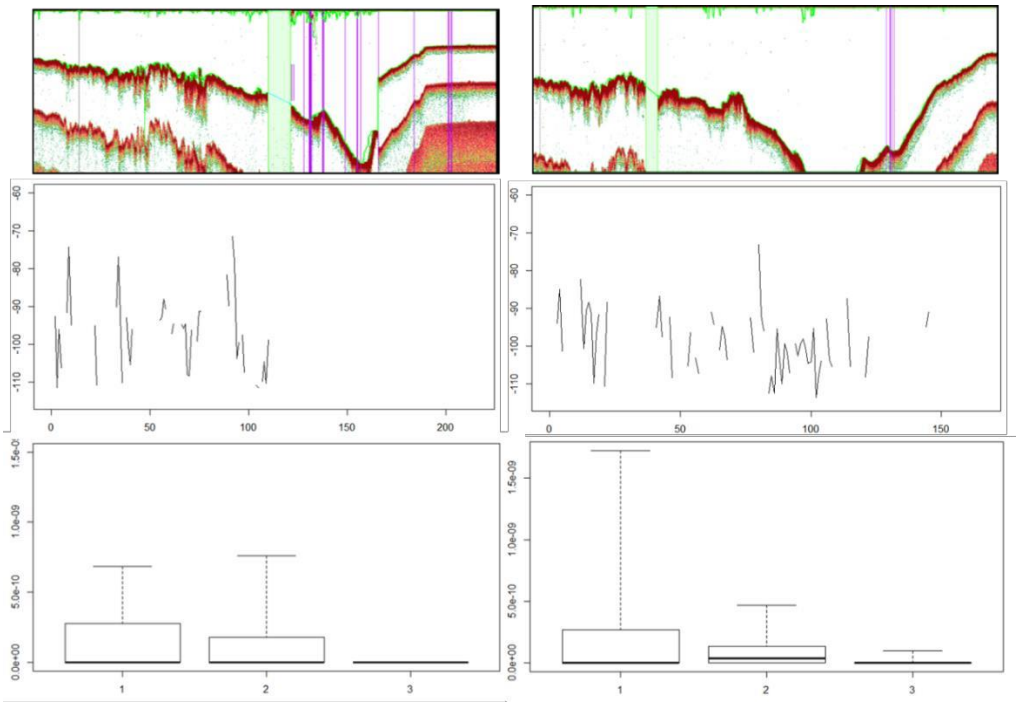

Figure A11: March survey, ebb tide grid 1 (left) and ebb tide grid 3 (right). Condensed echogram of cross-channel transects (top), mean relative fish density (middle) and boxplot of fish relative density (bottom). The purple vertical bars and area correspond to bad data and have not been echointegrated.

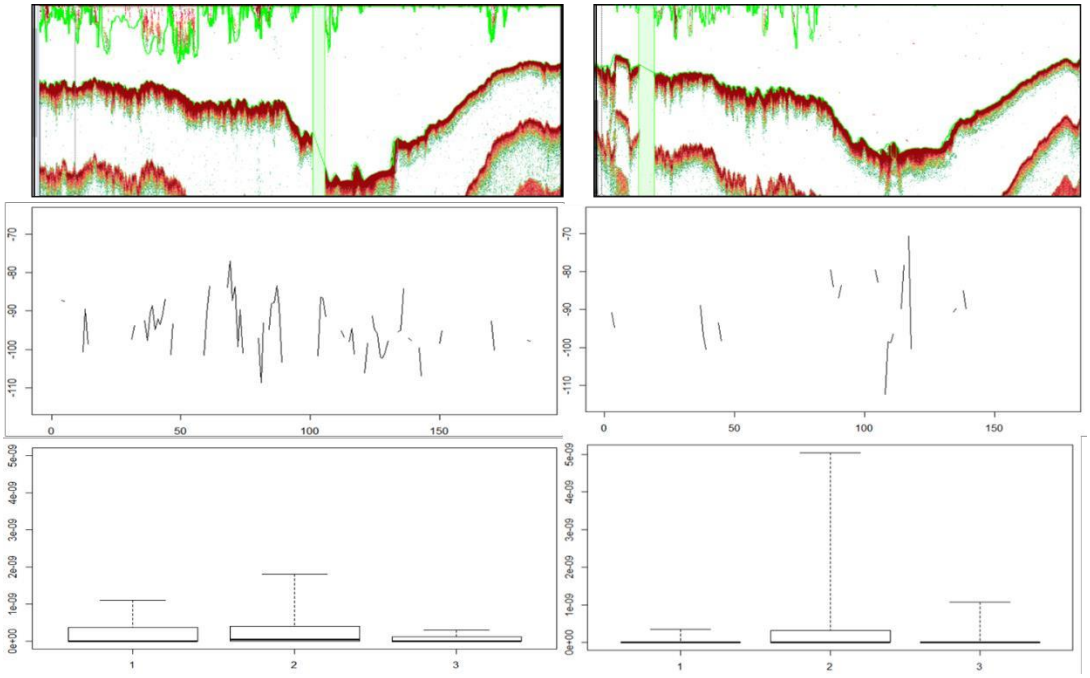

Figure A12: March survey, flood tide grid 2 (left) and flood tide grid 4 (right). Condensed echogram of cross-channel transects (top), mean relative fish density (middle) and boxplot of fish relative density (bottom). The purple vertical bars and area correspond to bad data and have not been echointegrated.